

Statistics of local temperature dissipation in high Rayleigh number convection

Emily S. C. Ching and C. Y. Kwok

Department of Physics, The Chinese University of Hong Kong, Shatin, Hong Kong

(Received 26 August 2000)

We study the statistics of the local temperature dissipation in high Rayleigh number convection. We find that its probability distribution deviates from a lognormal, although very low order moments can be approximated by a lognormal distribution. Instead, the moments satisfy a hierarchy similar to that proposed by She and Leveque [Phys. Rev. Lett. **72**, 336 (1994)] for the local energy dissipation. Moreover, the moments scale with the separation time. No change in the scaling behavior is observed when the Bolgiano scale is crossed, indicating that the statistics have the same nature in the buoyancy-driven and the inertia-driven regimes.

PACS number(s): 47.27.-i, 05.40.-a

High Rayleigh number convection has been a model system for studying turbulence. In thermal convection, the dynamics is driven by an applied temperature difference across the height of an experimental cell. In this sense, the temperature field is an active scalar. The flow state is characterized by the geometry of the cell and two dimensionless parameters: the Rayleigh number $Ra = \alpha g \Delta L^3 / (\nu \kappa)$ and the Prandtl number $Pr = \nu / \kappa$, where L is the height of the cell, Δ is the applied temperature difference, g the acceleration due to gravity, and α , ν , and κ are respectively the volume expansion coefficient, the kinematic viscosity, and the thermal diffusivity of the fluid. When Ra is large enough, the convection becomes turbulent.

The velocity field in high Reynolds number Navier-Stokes turbulence is intermittent and does not have self-similar statistics. The velocity structure functions $\langle [u(x+r) - u(x)]^p \rangle$ scale as r^{ξ_p} when r is within the inertial range but with exponents ξ_p deviating from $p/3$, the values predicted by the 1941 Kolmogorov theory [1]. Similarly, the fluctuating temperature field in turbulent convection has scale-dependent statistics and is intermittent [2]. A lot of work in turbulence research focuses on understanding the problem of intermittency: on understanding why simple dimensional arguments of the type presented in *K41* are not completely correct.

Kolmogorov's refined similarity hypothesis (RSH) [3] attributed the intermittency of the velocity field to the spatial variations of the energy dissipation by relating the velocity difference $u(x+r) - u(x)$ to the local energy dissipation ϵ_r , averaged over a ball of radius r for r within the inertial range. Kolmogorov further assumed that ϵ_r is lognormal and obtained explicit results for ξ_p . However, the lognormal model is known to have several shortcomings [4]. She and Leveque proposed a hierarchy for the moments of ϵ_r [5] which leads to good agreement with experiments. With RSH, this leads to a similar relation for the velocity structure functions.

Such hierarchical relation was shown to be naturally satisfied by log-Poisson statistics [6,7]. In addition to the local energy dissipation [8] and the velocity structure functions [9,10] in Navier-Stokes turbulence, the passive scalar structure functions [11] and the local passive scalar dissipation [12], the temperature structure functions in turbulent convec-

tion [13], and the velocity structure functions in a class of shell models [14–16] were all found to satisfy similar hierarchical relation.

In turbulent convection, besides the problem of intermittency there is also the issue of whether and how the characteristics of turbulence are affected by the presence of buoyancy. The mixing dynamics is expected to be driven by buoyancy for length scales $r > l_B$, where $l_B \equiv \bar{\epsilon}^{5/4} / [\bar{\chi}^{3/4} (\alpha g)^{3/2}]$ [17] is the Bolgiano scale. Here $\bar{\epsilon}$ and $\bar{\chi}$ are respectively the average energy and temperature dissipation rates. For $r < l_B$, it is expected that the inertial force of the fluid motion drives the mixing and the temperature is effectively passive. If buoyancy does affect the characteristics of turbulence, one expects that the statistical features of the temperature field would be different in the two regimes of length scales. Recently, one of us (Ching) has indeed found that the normalized temperature structure functions have different scaling exponents in the buoyancy-driven and in the inertia-driven regimes [13].

In our present project, we attempt to gain more understanding of the intermittency problem by separating it into two parts: the understanding of the conditional temperature structure functions at fixed values of the locally averaged temperature dissipation rate [18] and the understanding of the statistics of the local temperature dissipation. This separation allows us to particularly address the interesting question of whether RSH type ideas would be fruitful, that is, whether the intermittency of the temperature field can be attributed to the spatial variation of the temperature dissipation.

In this Rapid Communication, we report our study on the statistics of the local temperature dissipation in high Rayleigh number convection. In particular, we investigate whether the statistics can also be characterized by a hierarchical structure, and whether there is a change of behavior when the Bolgiano scale is crossed.

We use data from the well-documented Chicago experiment of low temperature helium gas [19,20] for our analyses. The experimental cell heated from below is cylindrical with a diameter of 20 cm and a height of 40 cm. A mean circulating flow is present for Rayleigh numbers larger than 10^8 . The temperature at the center of the cell, $T(t)$, was measured as a function of time t .

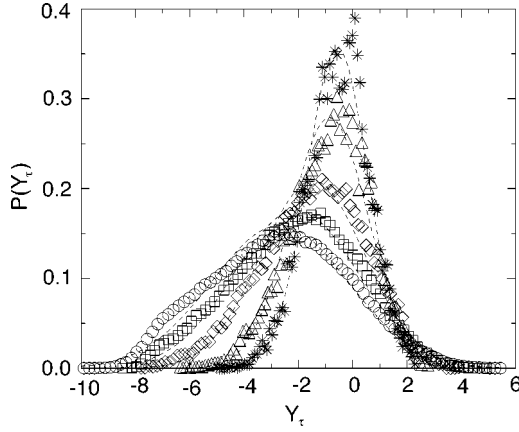


FIG. 1. Probability density functions of the logarithm of the normalized locally averaged temperature dissipation rate $P(Y_\tau)$ vs Y_τ for $\tau=8$ (circles), $\tau=32$ (squares), $\tau=128$ (diamonds), $\tau=512$ (triangles), and $\tau=1024$ (stars). All times are in units of the sampling time = 1/320 s. For comparison, Gaussian distributions with the same mean and standard deviation (dashed lines) are shown for each τ .

We define χ_τ by

$$\chi_\tau(t) \equiv \frac{1}{\tau} \int_t^{t+\tau} \frac{\kappa}{\langle u_c^2 \rangle} \left(\frac{\partial T}{\partial t'} \right)^2 dt', \quad (1)$$

where $\langle u_c^2 \rangle$ is the mean square velocity fluctuations at the center of the cell. We use χ_τ , which can be easily calculated using the one-point temperature measurements, to estimate the local temperature dissipation, which is the average of $\kappa |\nabla T|^2$ over a ball of size r .

The intermittency of the temperature field manifests itself as a τ -dependence of the probability density function (PDF) of $T_\tau \equiv T(t+\tau) - T(t)$. From this τ dependence, the dissipation and the circulation time scales, τ_d and τ_c , were identified [2]. In the present work, we study χ_τ for τ within the interval (τ_d, τ_c) , which corresponds to the inertial range. We focus on the data set taken at $Ra = 7.3 \times 10^{10}$, which has the longest scaling range both in the temperature frequency power spectrum [21] and in the generalized extended self-similarity plots of the temperature structure functions [13]. The sampling frequency is 320 Hz and the number of data points is 614 400. τ_d and τ_c are approximately 0.02 and 5.5 s, which are respectively 6 and 1750 sampling time intervals.

We shall first investigate the probability distribution of $\ln \chi_\tau$. Define

$$Y_\tau \equiv \ln \left(\frac{\chi_\tau}{\chi} \right), \quad (2)$$

where

$$\chi = \frac{1}{\tau_{total}} \int_0^{\tau_{total}} \frac{\kappa}{\langle u_c^2 \rangle} \left(\frac{\partial T}{\partial t} \right)^2 dt \quad (3)$$

and τ_{total} is the total measurement time. In Fig. 1, we show the PDFs of Y_τ , $P(Y_\tau)$, for various values of τ . It can be seen that $P(Y_\tau)$ depends on τ . The mean m_τ for all the PDFs is negative, implying that it is more probable for χ_τ to have

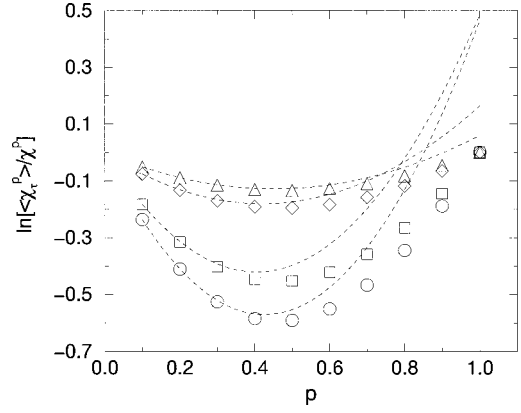


FIG. 2. Moments of $\langle \chi_\tau^p \rangle$ vs p for $\tau=8$ (circles), $\tau=32$ (squares), $\tau=128$ (diamonds), and $\tau=1024$ (triangles). All times are in units of the sampling time = 1/320 s. It can be seen that the lognormal approximation (dashed lines) is good only for small p .

values smaller than χ . m_τ increases to approximately zero while the standard deviation σ_τ decreases to approximately 1 as τ approaches τ_c . The PDFs are slightly asymmetric, and the kurtosis decreases from larger than 10 to around 3 as τ increases from τ_d to τ_c . For comparison, we also plot the Gaussian distributions with the same mean and standard deviation for each τ in Fig. 1. All the PDFs deviate from a Gaussian but the difference is smaller for larger τ , as reflected by the value of the kurtosis.

Although χ_τ is not lognormal, it would be useful to know how well the low order moments can be approximated by assuming Y_τ to be Gaussian. Suppose Y_τ were Gaussian with the same m_τ and σ_τ , the moments of χ_τ , $\langle \chi_\tau^p \rangle$, would be given by

$$\langle \chi_\tau^p \rangle_{\text{lognormal}} = \chi^p e^{m_\tau p + \sigma_\tau^2 p^2 / 2}. \quad (4)$$

As can be seen from Fig. 2, this approximation is only good when p is small. The maximum value of p such that the approximation is good increases as τ increases. In order for Eq. (4) to be a good approximation for the whole range of (τ_d, τ_c) , p has to be smaller than 0.2. Such a small value of p renders the lognormal approximation not useful for describing the dependence of the moments $\langle \chi_\tau^p \rangle$ on τ (see below).

Next, we address the question whether the moments of χ_τ satisfy the following hierarchy:

$$\frac{\langle \chi_\tau^{p+2q} \rangle}{\langle \chi_\tau^{p+q} \rangle} = A_{p,q} \left[\frac{\langle \chi_\tau^{p+q} \rangle}{\langle \chi_\tau^p \rangle} \right]^{\beta_\chi^q} \chi_\tau^{(q,\infty)1 - \beta_\chi^q}, \quad (5)$$

where

$$\chi_\tau^{(q,\infty)} \equiv \left[\lim_{p \rightarrow \infty} \frac{\langle \chi_\tau^{p+q} \rangle}{\langle \chi_\tau^p \rangle} \right]. \quad (6)$$

β_χ is a parameter between 0 and 1 for $p \geq 0$, and $A_{p,q}$ are constants independent of τ . Equation (5) is a generalization of the She-Leveque hierarchy [5] to any value of q not necessarily equal to 1. When long data sets are not available, as in the present work, one can check Eq. (5) without the need

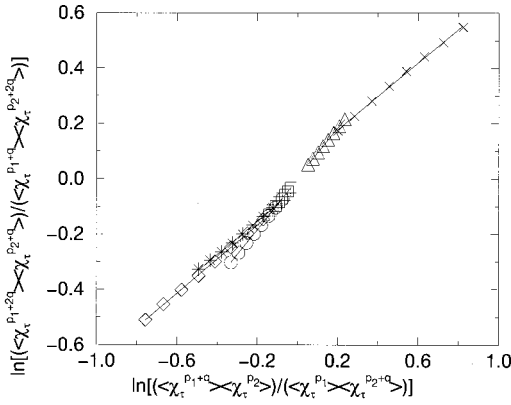


FIG. 3. $\ln(\langle\chi_\tau^{p_1+2q}\rangle\langle\chi_\tau^{p_2+q}\rangle)/(\langle\chi_\tau^{p_1+q}\rangle\langle\chi_\tau^{p_2+2q}\rangle)$ vs $\ln(\langle\chi_\tau^{p_1+q}\rangle\langle\chi_\tau^{p_2}\rangle)/(\langle\chi_\tau^{p_1}\rangle\langle\chi_\tau^{p_2+q}\rangle)$ for $p_1=0.1, p_2=0.8, q=0.1$ (circles); $p_1=0.3, p_2=0.6, q=0.1$ (squares); $p_1=0.7, p_2=0.2, q=0.1$ (triangles); $p_1=0.1, p_2=0.5, q=0.4$ (diamonds); $p_1=0.3, p_2=0.6, q=0.4$ (stars); and $p_1=0.7, p_2=0.2, q=0.4$ (crosses). The data points can be well fitted by straight lines (solid lines) indicating that the moments satisfy the hierarchical relation (5).

to calculate very high order moments by using a small value of q . We plot $(\langle\chi_\tau^{p_1+2q}\rangle\langle\chi_\tau^{p_2+q}\rangle)/(\langle\chi_\tau^{p_1+q}\rangle\langle\chi_\tau^{p_2+2q}\rangle)$ versus $(\langle\chi_\tau^{p_1+q}\rangle\langle\chi_\tau^{p_2}\rangle)/(\langle\chi_\tau^{p_1}\rangle\langle\chi_\tau^{p_2+q}\rangle)$ on a log-log scale by varying τ and keeping p_1, p_2 , and q fixed. If Eq. (5) is valid, a straight line with slope β_χ^q should be observed. Such plots for different values of p_1 and p_2 are shown in Fig. 3. Straight lines with the same slope are indeed observed for each q . The intercepts are close to zero, indicating that the constants $A_{p,q}$ are independent of p . The value of β_χ is found to be 0.31 ± 0.02 .

Finally, we study the dependence of $\langle\chi_\tau^p\rangle$ on τ . As shown in Fig. 4, $\langle\chi_\tau^p\rangle$ scales as τ^{μ_p} for τ within the range (τ_d, τ_c) . It is also clearly shown that the lognormal assumption (4) (dotted lines) fails to capture the τ dependence except for very small p . Using Eq. (5), the functional dependence of the scaling exponents μ_p on p is obtained as

$$\mu_p = c(1 - \beta_\chi^p) - \lambda p, \quad (7)$$

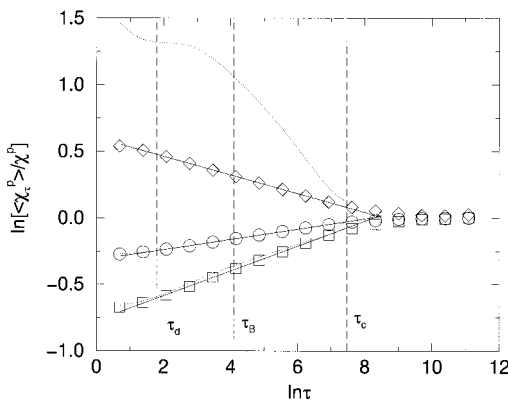


FIG. 4. Scaling behavior of $\langle\chi_\tau^p\rangle$ as a function of τ . The three time scales τ_d, τ_B , and τ_c are indicated by dashed lines. $p=0.1$ (circles), $p=0.4$ (squares), and $p=1.2$ (diamonds). The solid lines are power-law fits, while the dotted lines are the lognormal approximation, which is good only for $p=0.1$.

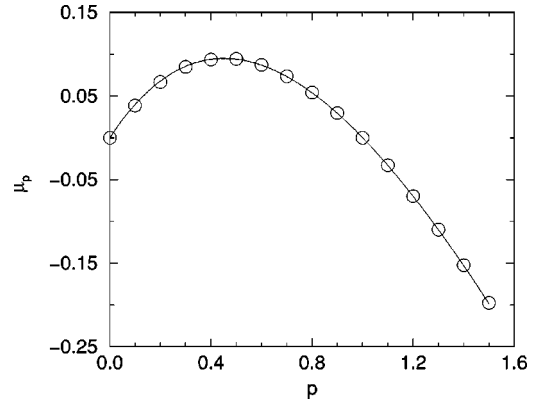


FIG. 5. Scaling exponents of μ_p as a function of p . The solid line is Eq. (8), using the fitted values of $\lambda=0.66$ and $\beta_\chi=0.31$.

where c and λ are two parameters. It is straightforward to see that $\langle\chi_\tau\rangle = (1/\tau_{total}) \int_0^{\tau_{total}} \chi_\tau(t) dt$ is approximately equal to χ for τ small compared to τ_{total} . Thus, $\langle\chi_\tau\rangle$ is independent of τ and $\mu_1=0$. Hence, Eq. (7) becomes

$$\mu_p = \lambda \left[\frac{1 - \beta_\chi^p}{1 - \beta_\chi} - p \right]. \quad (8)$$

Equation (8) implies that

$$\chi_\tau^{(q,\infty)} \sim \tau^{-\lambda q}. \quad (9)$$

Thus, the parameter λ is the negative of the scaling exponent of $\chi_\tau^{(1,\infty)}$. We plot $(\langle\chi_{\tau_1}^{p+2q}\rangle\langle\chi_{\tau_2}^{p+q}\rangle)/(\langle\chi_{\tau_1}^{p+q}\rangle\langle\chi_{\tau_2}^{p+2q}\rangle)$ versus $(\langle\chi_{\tau_1}^{p+q}\rangle\langle\chi_{\tau_2}^p\rangle)/(\langle\chi_{\tau_1}^p\rangle\langle\chi_{\tau_2}^{p+q}\rangle)$ on a log-log scale by varying p and keeping τ_1, τ_2 , and q fixed. Straight lines with slope β_χ^q are again observed, and the intercepts are $-\lambda q(1 - \beta_\chi^q) \ln(\tau_1/\tau_2)$. The estimated value of λ is 0.66 ± 0.02 . In Fig. 5, we show the exponents μ_p and compare them with Eq. (8) using the estimated values of β_χ and λ (solid line). Good agreement can be seen, further verifying Eq. (5).

It was shown [22] that l_B can be written as

$$l_B = \frac{\text{Nu}^{1/2} L}{(\text{Ra Pr})^{1/4}}, \quad (10)$$

where the Nusselt number (Nu) is the heat flux normalized by that when there was only conduction. A time scale corresponding to l_B can be naturally defined as $\tau_B = \tau_c l_B / L$ and is easily evaluated using the measured values of Nu, Ra, and Pr. For $\text{Ra} = 7.3 \times 10^{10}$, $\tau_B \approx 60$ sampling time intervals. In Fig. 4, we see that the scaling behavior of $\langle\chi_\tau^p\rangle$ extends over approximately the whole range of (τ_d, τ_c) with no observable change when τ_B is crossed. This suggests that the statistics of χ_τ have the same nature in the two regimes of scales. This further suggests that the statistics of χ_τ have the same nature no matter whether the temperature field acts as an active scalar or is effectively passive.

Finally, it is interesting to see what values of c, λ , and β_χ would be given by simple phenomenology and dimensional arguments. Dimensionally, $\chi_\tau^{(1,\infty)}$ is a temperature variance divided by a time. The maximum temperature variance is Δ^2 . So, we take $\chi_\tau^{(1,\infty)} \sim \Delta^2/t_\tau$, where $t_\tau \sim r/u_r$ is the eddy turn-

over time at the scale $r = \langle u_c^2 \rangle^{1/2} \tau$. In the inertia-driven regime, one expects u_r to be given by the average energy dissipation rate: $u_r \sim (r\bar{\epsilon})^{1/3}$, which gives $\chi_\tau^{(1,\infty)} \sim \tau^{-2/3}$. Thus $\lambda = 2/3$, which is very close to what we have found. On the other hand, when buoyancy is important, one would expect u_r to be related to the buoyancy term: $u_r^2/r \sim (\alpha g) T_r$, where T_r is the temperature difference across the scale r and is expected to be related to the average temperature dissipation rate: $T_r^2 u_r / r \sim \bar{\chi}$. In this case, $\chi_\tau^{(1,\infty)} \sim \tau^{-2/5}$ and λ would be $2/5$, which is not observed. Instead, we have just seen that λ is close to $2/3$ for the whole range (τ_d, τ_c) . The value of c can be interpreted as the co-dimension of the most dissipative structures. For the passive scalar, numerical simulations suggest that such structures are sheetlike, giving $c = 1$. Using $\lambda = 2/3$ and $c = 1$, $\mu_1 = 0$ gives $\beta_\chi = 1/3$, which is again close to what we have found.

In summary, we have carried out a systematic study on the statistics of the local temperature dissipation, estimated by χ_τ , in turbulent convection. We have found that the PDF of χ_τ depends on τ and is not lognormal, even though very low order moments can be approximated by assuming that it

is lognormal. Instead, the moments satisfy a hierarchical structure of the form similar to that proposed by She and Leveque for the local energy dissipation. Moreover, $\langle \chi_\tau^p \rangle$ scale as τ^{μ_p} for $\tau_d < \tau < \tau_c$, and the scaling exponents μ_p have the functional dependence (8) implied by the hierarchical structure. No change in the scaling behavior is observed when the scale τ_B is crossed, indicating that the statistics of χ_τ have the same nature in the inertia- and buoyancy-driven regimes. This is somewhat surprising, as simple phenomenology would suggest different scaling behavior in the two regimes. This observation also implies that the change in the scaling exponents of the normalized temperature structure functions observed in Ref. [13] is solely the result of a change in the conditional temperature structure functions at fixed values of χ_τ . Such a change is indeed found, and the results are reported elsewhere [18].

This work is supported by a grant from the Research Grants Council of the Hong Kong Special Administrative Region, China (RGC Ref. No. CUHK 4119/98P).

-
- [1] A. N. Kolmogorov, C. R. Acad. Sci. URSS **30**, 301 (1941).
 [2] E. S. C. Ching, Phys. Rev. A **44**, 3622 (1991).
 [3] A. N. Kolmogorov, J. Fluid Mech. **12**, 82 (1962).
 [4] U. Frisch, *Turbulence: The Legacy of A. N. Kolmogorov* (Cambridge University Press, Cambridge, England, 1995).
 [5] Z.-S. She and E. Leveque, Phys. Rev. Lett. **72**, 336 (1994).
 [6] B. Dubrulle, Phys. Rev. Lett. **73**, 959 (1994).
 [7] Z.-S. She and E. C. Waymire, Phys. Rev. Lett. **74**, 262 (1995).
 [8] G. Ruiz-Chavarría, C. Baudet, and S. Ciliberto, Phys. Rev. Lett. **74**, 1986 (1995).
 [9] G. Ruiz-Chavarría, C. Baudet, R. Benzi, and S. Ciliberto, J. Phys. II **5**, 486 (1995).
 [10] R. Camussi and R. Benzi, Phys. Fluids **9**, 257 (1997).
 [11] G. Ruiz-Chavarría, C. Baudet, and S. Ciliberto, Physica D **99**, 369 (1996).
 [12] E. Leveque, G. Ruiz-Chavarría, C. Baudet, and S. Ciliberto, Phys. Fluids **11**, 1869 (1999).
 [13] E. S. C. Ching, Phys. Rev. E **61**, R33 (2000).
 [14] P. Frick, B. Dubrulle, and A. Babiano, Phys. Rev. E **51**, 5582 (1995).
 [15] R. Benzi, L. Biferale, and E. Trovatore, Phys. Rev. Lett. **77**, 3114 (1996).
 [16] E. Leveque and Z.-S. She, Phys. Rev. E **55**, 2789 (1997).
 [17] A. S. Monin and A. M. Yaglom, *Statistical Fluid Mechanics* (MIT Press, Cambridge, MA, 1975).
 [18] E. S. C. Ching and K. L. Chau (unpublished).
 [19] F. Heslot, B. Castaing, and A. Libchaber, Phys. Rev. A **36**, 5870 (1987).
 [20] M. Sano, X.-Z. Wu, and A. Libchaber, Phys. Rev. A **40**, 6421 (1989).
 [21] X.-Z. Wu, L. Kadanoff, A. Libchaber, and M. Sano, Phys. Rev. Lett. **64**, 2140 (1990).
 [22] F. Chiliá, S. Ciliberto, C. Innocenti, and E. Pampaloni, Nuovo Cimento D **15**, 1229 (1993).